



EVIDENCE FOR REAL-TIME CORRELATION OF MINING ACTIVITY AND INDUCED EARTHQUAKES IN PARNASSOS MINE (GREECE)

Chrisanthi VENTOUZI¹, Constantinos PAPAACHOS², Domenikos VAMVAKARIS³, Iordanis DIMITRIADIS⁴ and Athanasios KARAMEISINIS⁵

SUMMARY

A study of the microearthquake activity observed at the Kaniani-Parnassos mines has performed in order to determine the origin of the several “unknown” shocks observed at the area of the mine. Preliminary analysis of the recordings indicated that the shocks were of tectonic origin. A portable network of three accelerographs (located inside the mine - no absolute time) and five three-component digital seismographs (located in surface locations on top of the mine - absolute time available) were installed for a period of nine months. The analysis of impulsive, high frequency (>20 Hz), short duration (2-3 sec) recordings, showed that the observed seismicity is of very local scale, located at a specific section of the mine.

The microseismic activity exhibited a very strong time-correlation with the exploitation level, as this is revealed from the very significant variation of the earthquake rate of occurrence after the start of the operation of the mine, as well as the clear coupling on the rate of microearthquake occurrence with the rate of mining explosions. The focal mechanisms of the ruptures and the local stress field were evaluated using the first arrivals of the P-waves along with the P/S spectral ratios. The focal mechanisms are all of thrust type, indicating reverse ruptures caused by a compressional stress field with ESE-WSW direction. This field is almost perpendicular to the strike of the local old syncline-anticline, where the mine deposit is located; hence it can be safely assumed that is the “remnant” stress field that created this compressional mega-structure. The determined ruptures are in excellent agreement with the main tectonic discontinuities mapped inside the mine. A typical dynamic stress drop of 10-20 bars was also calculated for the biggest events ($M \sim 1$) which is relatively comparable with the typical expected value of the mean effective isotropic stress (~ 50 bars).

1. INTRODUCTION

The Parnassos mine is one of the most important sources of bauxite deposits in Greece. The mines at were established in 1933 for the exploitation of the bauxite at the mountains of Parnassos, Ghiona and Iti. Parnassos bauxite is mined in the mountain region of Parnassos and Ghiona at an average altitude of 800m. The ore is extracted by surface and underground mining by the method of room and pillar. The room and pillar mining involves driving tunnel-like openings to divide the ore seam into rectangular or square blocks. These blocks of

¹ Department of Geophysics, School Geology, Aristotle University of Thessaloniki, GR 54124 Theesaloniki, Greece
Email : xrusven@geo.auth.gr

² Department of Geophysics, School Geology, Aristotle University of Thessaloniki, GR 54124 Theesaloniki, Greece
Email : kpapaza@geo.auth.gr

³ Department of Geophysics, School Geology, Aristotle University of Thessaloniki, GR 54124 Theesaloniki, Greece
Email : dom@geo.auth.gr

⁴ Department of Geophysics, School Geology, Aristotle University of Thessaloniki, GR 54124 Theesaloniki, Greece
Email : iordanis@geo.auth.gr

⁵ Department of Geophysics, School Geology, Aristotle University of Thessaloniki, GR 54124 Theesaloniki, Greece
Email : akarames@geo.auth.gr

ore or pillars are sized to provide support of the overlaying strata, while the openings are referred to as rooms or entries.

Very often mining is accompanied by the occurrence of numerous induced seismic events. The existence of such seismic events is well known all over the world and has been investigated from many researchers [Kijko, 1985; Gibowicz, 1990]. This type of seismic activity observed in a mine alternates between periods of high exploitation and more “calm” periods with less ore extraction rate (Zhong et al, 1997). These shallow earthquakes have simple waveforms, well determined surface waves, high frequencies with long periods and slow decrease of their amplitude. These events occur, as mentioned, due to the extraction of the deposit and the artificial explosions in the areas where the most intense exploitation is taking place. The occurrence of mine-induced seismic events can be of many different modes, such as fault slip, rockburst, pillar burst, bump and outburst (Hasegawa et al, 1989). Faulting can also occur near the stope face which is being mined [Cook, 1963; McGarr, 1971] and at places in the mine where volume closure is occurring at a high rate, and either above or below the mine along weakened faults [Hinzen, 1982; Smith et al., 1974].

The purpose of this study is the determination of the sources of the microshocks observed at the area of Kaniani mines on Parnassos mountain, exploited by S&B Mining Company. The above determination included the territorial location of the sources of these unusual tremors and their focal mechanisms (if they are of tectonic origin), in order to define the local stress field that causes them. The description of this activity consisted of the following stages: a) Analysis of the important recordings of the existing vibration monitor instrument (spectral analysis, polarization analysis, calibration of the propagation medium from artificial explosions), b) Installation of a five seismographs (surface) and three accelerographs (inside the mine) network along with an existing vibration monitor instrument, c) Analysis of the recordings, determination of the sources, definition of the focal mechanisms in case of events of tectonic origin, calibration of the recording instruments with the use of the artificial explosions and d) Determination of the local stress field from the local events and their epicentral distribution.

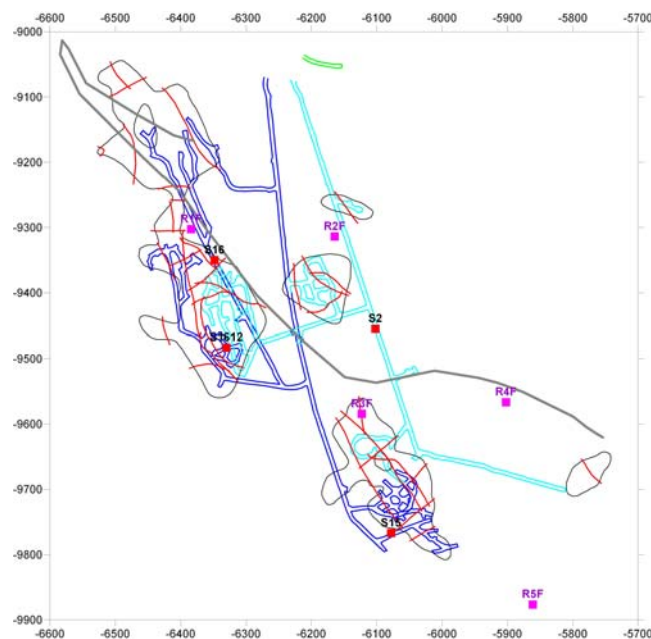


Figure 1: Distribution of the seismographs (purple squares) and the accelerographs (red squares) installed in the “Tsakni-Mantri” area. With the grey line the access road to the mines is presented, while the red line depicts the main observed underground tectonic discontinuities in the exploitation areas.

2. OBSERVATION OF THE MINING SEISMIC ACTIVITY

A portable network of five three-component digital seismographs places was installed in order to study the seismicity observed at the area of the bauxite exploitation. In addition to the five station network of seismographs, three accelerographs were installed inside the mine for a more effective monitoring of the study area. It should be mentioned that the accelerographs were regulated to the highest level of sensibility

(STA/LTA:2) in order to record even weak ground motions that sometimes barely exceed the noise level from natural or man-made sources. The distribution of the seismographs and accelerographs is shown in Figure 1.

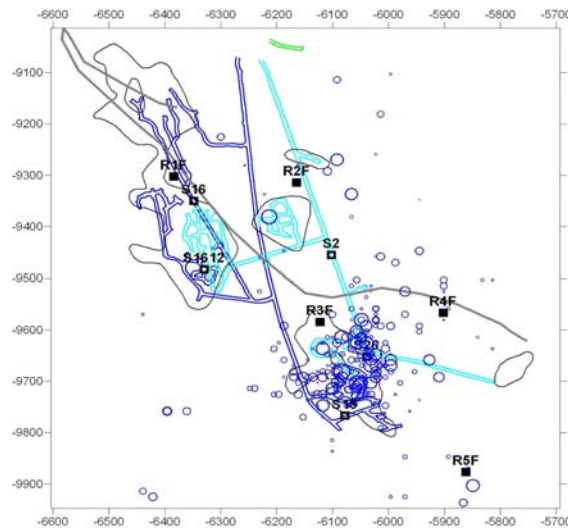


Figure 2: Epicentral distribution of the events recorded in the area of the mines for the period the network was installed according to their moment magnitude. The activity is concentrated in one region (S1.3) where the exploitation of the ore is taking place almost exclusively.

The network was in continuous operation for a period of 9 months (May 2005 to January 2006). Within this period all the available data were studied in detail. The waveforms from the records were carefully viewed in order to locate the events and the seismic arrivals. The location of these impulsive, high frequency (>20 Hz), short duration (2-3 sec) recordings allowed the study of their epicentral distribution. Based on the available data, after the calibration of the instruments, a calculation of the seismic-moment magnitudes was performed for all earthquakes that were recorded from the microseismic network. The typical error in the determination of the moment magnitude was below 0.2, which is relatively small compared with the usual determination error (~0.3). The recorded magnitudes vary between $M=-2.0$ and $M=1.5$, which corresponds to the strongest event recorded (30 October 2005). All events are presented in Figure 2 according to their moment magnitude.

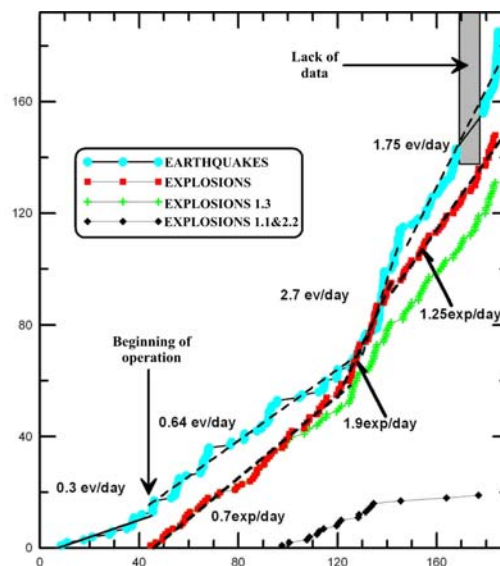


Figure 3: Time variation of the cumulative number of the events (blue circles) and the exploitation explosions (red squares) until November 1 as a function of time, which is presented in days after May 1. The changes in the event rate (seismicity level) and explosion rate (intensity of exploitation) are also shown. The initial stabilization and possible reduction of the seismotectonic activity for the period July 8-September 2 and the subsequent increase of the activity as a result of the increase of the number of explosions, as well as the reestablishment into more normal rates of seismicity after October 25 as a result of the decrease of the exploitation is clear.

The mean typical (mathematical) travel-time RMS errors was about 2msec and the corresponding mean typical error for the epicentral determination was of the order of 10m. Therefore, it can easily be concluded that the majority of the recorded events had actual location errors less than 20-40m. The mean value of the number of phases used for the process of the data was eight for each event, while the mean depth of the shocks was found to lie at the altitude of 500-550m. Even though the error at the determination of the depth was significantly higher, the recorded events were not deep tectonic shocks (e.g. 1km under the mines), but events that occurred very close to the exploitation level. In any case the accuracy in the determination of the epicentres was quite high (<50-100m), hence there was no doubt about the spatial location generating these tectonic events.

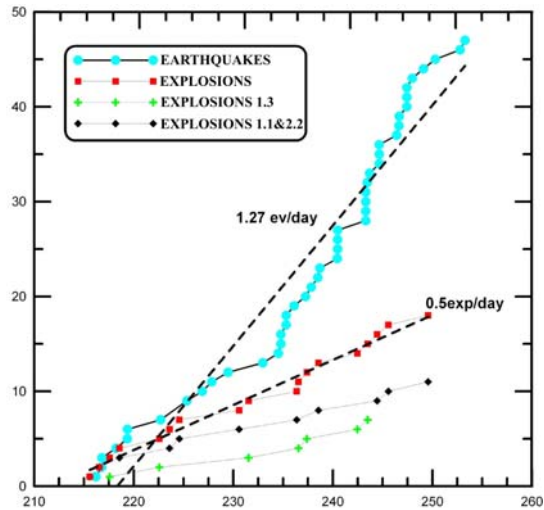


Figure 4: Time variation of the cumulative number of the events (blue circles) and the exploitation explosions (red squares) for the period December 2 2005-January 9 2006 as a function of time, which is presented in days after May 1.

After the beginning of the operation of the mine (15 June) it was very important to discover whether the operation of the mine affected the generation of the tectonic events in the area of the mines and if this influence exhibited specific characteristics (stable rate or gradual reduction of the induced activity) or revealed features which could probably cause an increased (accelerating) activity, leading to the generation of stronger events. The cumulative number of earthquakes that occurred in the area of the mines, as well as the cumulative number of artificial explosions are shown in figures 3 and 4. It is clear that after the start of the operation of the mine there was an increase of 2.5-3 times of the rate of tectonic events in the area of the mine and in particular at the area S1.3 where the main exploitation took place. The generation of these events appears in dense (space-time) groups, not directly connected with the explosions, although in some cases shocks were observed immediately after the explosions. The increase of the rate of birth of the tectonic events and their spatial distribution in the exploitation area, suggests the direct connection of the tectonic activity observed in the mine area and the exploitation of the mine. On July 7 at 20:31 a strong event occurred of seismic moment magnitude $M_w=0.9$, which was followed from many small “aftershocks”. The strongest one occurred about 11sec later. The waveform of this event recorded by the vibration monitor instrument (horizontal component) is shown in figure 5 along with the corresponding diagrams of the particle motion. The fitting of the displacement waveform spectrum is presented in figure 6 in order to determine the main source parameters (seismic moment, corner frequency, etc.).

In the interval July 8-September 2 the situation was stable and some gradual decrease of the activity was observed, which does not seem to be related with corresponding reduction of the frequency of the explosions (intensity of exploitation). This fact was an indication for stabilization or even abatement of the situation “simulated” by the initiation of the operation of the mine. The above state abruptly changed in September with the increase of the number of explosions of about 170% (from ~0.7 explosion per day to ~1.9 explosions per day), as shown in the corresponding curve (red squares) in figure 3. This increase resulted in a corresponding intense increase of the number of tectonic events (blue circles in Figure 3). The epicentral distribution of these events reveals that these shocks occurred in the same space (area S1.3) where the most intense exploitation was taking place. Following this phase, a decrease is observed in the number of the explosions, which corresponds to reduction of the exploitation rate to about 1.25 explosions per day, until the end of November 2005. This led up to a gradual decrease of the induced events, (~1.75 events per day or less), with some increase at the end of this

period, when the number of explosions increased. Hence, the initial assessment for a strong correlation of exploitation levels and induced seismicity was verified, with the generation rate of the tectonic events being almost proportional to the intensity of exploitation, although increase of the rate does not seem to result necessarily to an accelerating-critical behaviour of the induced microseismic activity.

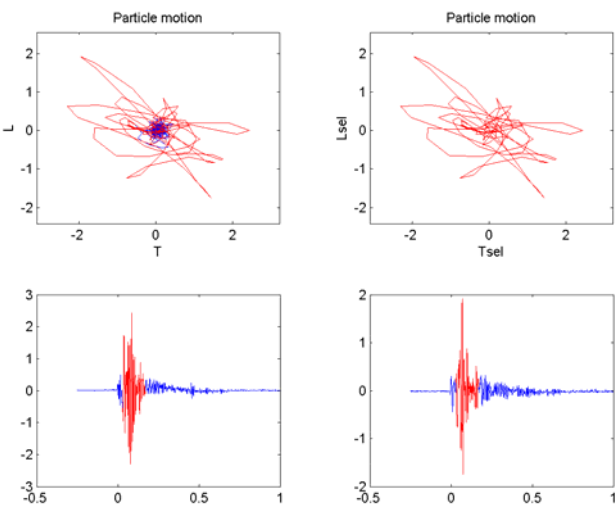


Figure 5: Seismic particle motion (up) and the corresponding horizontal components (down) from the vibration monitor instrument of the S&B Mining Company of the seismic event which occurred on July 7 20:31GMT with magnitude $M_w=0.9$

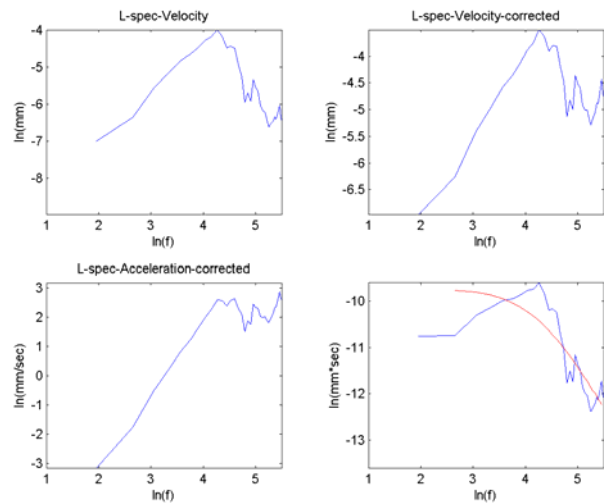


Figure 6: (up) Longitudinal (L) spectrum of the recording in S2 location from the vibration monitor system of Instantel Blastmate II type of the July 7 event before (left) and after (right) the correction for the anelastic attenuation (Q-factor). (down). Acceleration spectrum (left) and displacement spectrum (right) after the correction for the anelastic attenuation. For the displacement spectrum the red line marks the theoretical point source spectrum, which correspond to a seismic moment magnitude $M_w=0.9$ event.

It should be reported that a gap exists in the observation data of the seismic sequence for the period 16-25 October 2005 due to a malfunction of three seismographs. This gap does not significantly affects the pattern of Figure 3 (or Figure 1), and for this period it was assumed (for presentation needs) that the seismicity rate remained unchangeable.

3. LOCAL STRESS FIELD AND POSSIBLE FOCAL MECHANISM OF THE MICROEARTHQUAKES

Focal mechanism of the ruptures and the relative stress field that causes these ruptures was evaluated from the experimental data. The data analysis was based not only on the first arrivals of the preliminary (P) waves, but on the spectral ratios of the S/P recordings to different seismographs as well, allowing the reliable evaluation of the focal mechanisms from the relatively small number of observations. Nevertheless it should be noted that even with the use of the above approach, a large number of focal mechanisms of strong events (clear first arrivals) resulted in multiple solutions, hence a single kinematic axes configuration could not be determined. This is mostly due to the high uncertainty in depth estimation of the events. However, for a small number of strong events it was possible to determine reliable fault plane solutions.

In Figure 7 the focal mechanism (in stereographic projection) of the strong earthquake recorded in the mine area on July 7 is presented. The focal mechanism and the relative stress of this event are typical and almost identical with all the other focal mechanisms and stresses estimated. According to these results it can be safely argued that the ruptures are of reverse type (and not normal as was expected from the regional tectonic environment of the broader Parnassos area), caused by a compressional stress field with ENE-WSW direction. This field is almost perpendicular to the strike of the local old syncline-anticline, where the mine deposit is located; hence it can be safely assumed that this is the “remnant” stress field that created this compressional mega-structure. This statement is also supported by the fact that the active tectonic stress field in the broader region of Central Greece is tensional (not compressional) with almost E-W direction. Therefore even though it's not possible seismologically to determine which from the two planes of the focal mechanism is the main one, the position of the focal mechanism to the local anticline manifests that the plane with NNW-SSE direction which dips to the ENE direction is the main plane of the rupture (continuous line), while the plane with NE-SW direction is the secondary plane (dashed line). This statement is in excellent agreement with the main tectonic features with exactly the same direction (red lines in Figure 7), which are much more abundant and developed in length than the tectonic features with ENE-WSW direction.

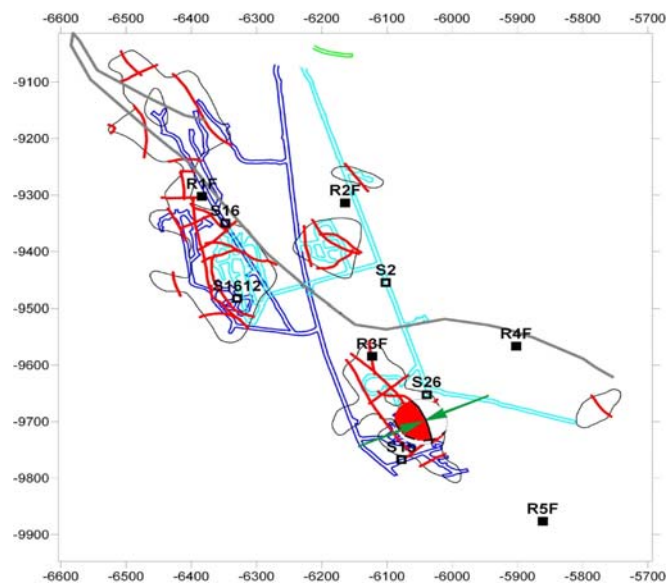


Figure 7: Stereographic projection of the earthquake recorded on July 7 and the compressional stress field.

The Gutenberg-Richter curve of the whole data set is presented in Figure 8. The upper horizontal axis represents the corresponding estimated rupture length. It is observed that the minimum completeness magnitude is $M \sim 1.3$ (all events recorded are above this magnitude) and corresponds to ~ 3 m of rupture length. The well-known linear Gutenberg-Richter relationship is fulfilled for events with larger magnitude. For magnitudes $M \geq 0.5$ (rupture length ~ 25 m) a saturation phenomenon appears, which means that the appearance of such ruptures is not “favored” by the “available” lengths of the existing tectonic discontinuities which slip due to the local stress field. This manifests that even if the visible rupture lengths possibly are larger than 150 m, the maximum slip occurs to sections of about 80 m length.

In Figures 9 and 10 (equivalent with Figures 3 and 4) the cumulative Benioff deformation (which is equal with the square root of the released energy and can be considered as the most reliable measure of deformation) is shown, in comparison with the number of earthquakes presented in Figures 3 and 4, since such plots also take into account the magnitude of the recorded events as well and not only their number.

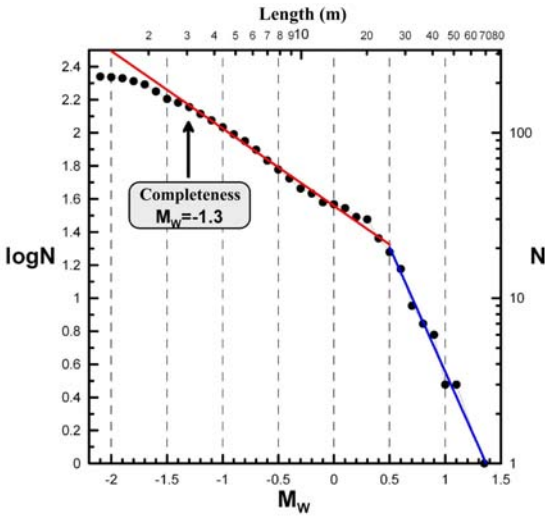


Figure 8: Gutenberg-Richter distribution of the all events recorded in the “Tsakni-Mantri” mining area. It is obvious that a linear relationship applies (as expected) from the minimum magnitude of completeness ($M \sim -1.3$) up to $M \sim 0.5$. For events with larger magnitudes a magnitude “saturation” is observed, which suggests an inability of the medium to be driven into very large ruptures.

From the spectral analysis a typical dynamic stress drop of 10-20bars was calculated for the biggest events ($M \sim 1.0$), while for the smaller events ($M \sim 0$) the calculated stress drop was of the order of ~ 3 -10bars. For smaller events the expected corner frequency is in practice out of the recorded spectrum and the corresponding value cannot be estimated. However, this was not so important because of their small magnitude. The observed stress drop is relatively comparable to the expected value of the mean effective isotropic stress (~ 50 bars).

There are remarkable differences in the values of corner frequencies to the area in which a mine is established. According to the calculations the events in Parnassos mines have magnitudes from $M = -2.0$ to $M = 1.5$ which correspond to seismic moment of about 10^6 Nm and 10^{11} Nm, respectively (Hanks and Kanamori, 1979), while the corner frequencies are ~ 70 Hz for $M = 1.5$ events and ~ 150 Hz for $M \sim 0$ events. In general, it has been observed that for the same values of corner frequencies different values of stress drop have been observed world-wide, depending on the location of the mine and especially on the main rock formation of the mine and its level of tectonic fragmentation. In regions where the medium around the active stope is composed of intact rock, not highly fractured and consists of hard rock (quartzite), the observed values of the stress drop are high (as in Parnassos mines ~ 10 bars) and the corresponding seismic moment magnitudes are quite large. On the contrary in mines where the rock mass is highly fractured or composed of not well connected rocks (sandstone) the observed stress drop is usually smaller (Gibowicz, 1995). Therefore the dependence of the stress drop with the seismic moment is apparent and of indicative nature.

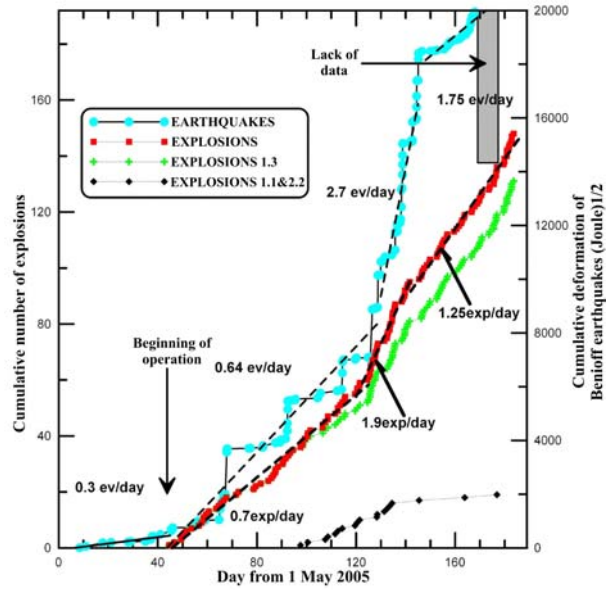


Figure 9: Time variation of the cumulative Benioff deformation of the events (blue circles) and the cumulative number of explosions (red squares) until November 1 as a function of time which is presented in days after May 1. The changes in the explosion rate (intensity of exploitation) are also shown. Similar conclusions with figure 3 can be drawn.

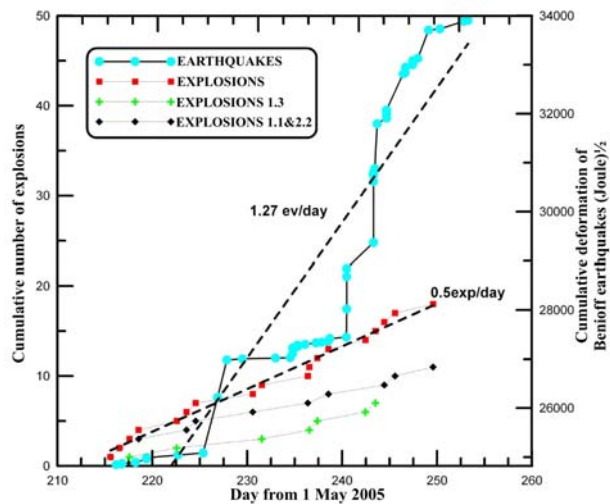


Figure 10: Time variation of the cumulative Benioff deformation of the events (blue circles) and the cumulative number of explosions (red squares) for the period December 2 2005-January 9 2006 in relation with time, which is presented in days after May 1.

4. DISCUSSION AND CONCLUSIONS

On the basis of all the available data it can be safely concluded that the observed seismicity is of local scale and is not related with the general seismotectonic activity of the area of Parnassos. Even though the errors in depth determination are bigger from the corresponding horizontal errors, they are located near the exploitation depth.

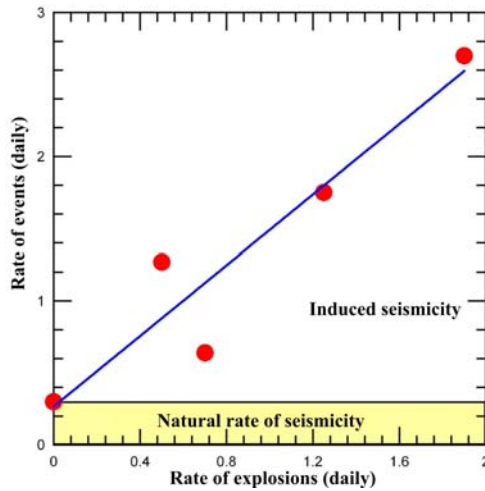


Figure 11: Daily variation of the number of occurrence of events in relation with the daily rate of explosions. It's clear the almost linear correlation with the increase of the daily rate of earthquakes of about 1.2 for each unit of increase of the daily rate of explosions.

The observed seismicity is directly related and affected by the exploitation as this was revealed from: 1) The intense increase of induced events after the initiation of the exploitation, 2) The almost complete correlation of its changes with the exploitation rate. This fact is described quantitatively in Figure 11 where the daily rate of explosions is correlated with the corresponding generation rate of the tectonic events. It should be pointed out that the intense exploitation resulted to particularly significant increase of the shocks, with a small delay of few days. The magnitude of the induced events does not appear to have a clear correlation with the exploitation rate, as is shown in Figure 12 and 13, where the mean magnitude of the earthquakes is also presented and which remains stable and uncorrelated with the exploitation rate after the initial rise (due to the start of the exploitation).

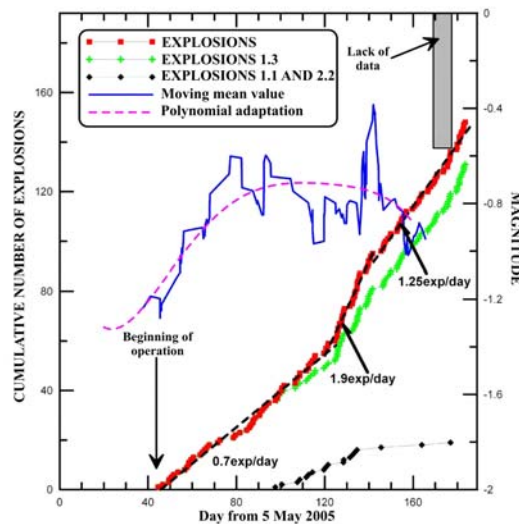


Figure 12: Time variation of the mean magnitude of the vents (blue line and pink dashed line) and of the cumulative number of explosions (red squares) until until November 1 as a function of time which is presented in days after May 1. An initial increase of the induced event magnitude (from ~ -1.3 to ~ -0.8) after the start of the exploitation is observed, while a more or less stable mean magnitude is observed for the remaining period suggesting that the intensity of the exploitation affects the number of the events but not their mean magnitude.

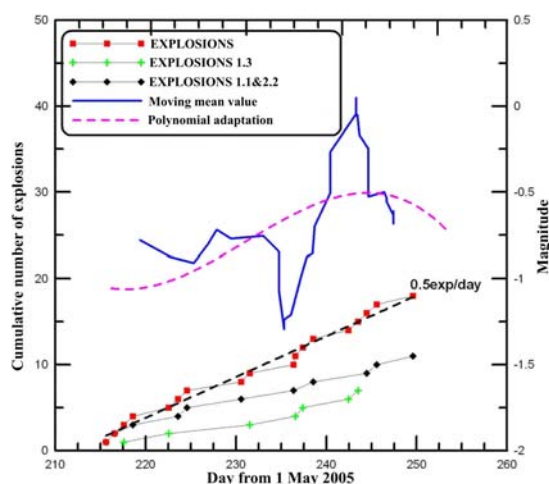


Figure 13: Same as fig. 12 for the time period November 1-January 9.

The activity is located almost exclusively confined in area S1.3, where the vast majority of the induced events occurred. Exploitation in other areas did not cause any intense seismicity in these or the surroundings sections of the mine, even in periods (see Figure 3) where the intensity of the explosions was higher in these places.

This induced seismicity seems to be caused from a remnant compressional stress field, similar with the one that caused the syncline-anticline system where the bauxites are found (compression with ENE-WSW direction). The possible strikes of the induced ruptures are of NNW-SSE direction, in excellent agreement with the observed main tectonic discontinuities mapped inside the mine. The typical dynamic stress drop of the strongest events is of the order of 10bars. Hence, it can be argued that the unloading of the S1.3 region due to the exploitation leads to the activation of the existed reverse ruptures from the remnant compressional stress field of the syncline-anticline, which for local reasons (local field anisotropy, discontinuity distribution, etc.) appear only in the specific area.

ACKNOWLEDGEMENTS

This work has been partly supported by Research Committee Aristotle Univ. Thessaloniki project 80588.

5. REFERENCES

- Gibowicz, S. J. (1990), The mechanism of seismic events induced by mining-a review in Rockbursts and Seismicity in Mines, *C. Fairhurst (editor)*, Balkema, Rotterdam, 3-28
- Hanks, T. C., and Kanamori, H. (1979), A moment magnitude scale, *J. Geophys. Res.*, 84, 2348-2350
- Hasegawa, H. S., Wetmiller, P. J., nad Genzwill, D. J. (1989), Induced seismicity in mines in Canada-An overview, *Pure and Appl. Geophys.*, 129, 423-453
- Hinzen, K. G. (1982), Source parameters of mine tremors in the eastern part of Ruhr-District (West Germany), *J. Geophys.*, 51, 105-112
- Kijko, A. (1985), Theoretical model for a relationship between mining seismicity and excavation area, *Acta Geophys. Pol.*, 33, 231-242
- McGarr, A. (1971), Violent deformation of rock near deep-level, tabular excavations-seismic events, *Bull. Seism. Soc. Am.*, 61, 1453-1466
- Smith, R. B., Winklers, P. L., Anderson, J. G., and Scholz, C. H. (1974), Source mechanisms of microearthquakes associated with underground mines in eastern Utah, *Bull. Seism. Soc. Am.*, 64, 1295-1317
- Zhong, Y. Z., Gao, G., and Yun, B. (1997), Induced seismicity in Lianonig Province, Cina, *Pure and Appl. Geophys.*, 150, 461-472